Upgraded formulation of the nuclear eigenvalue problem in a microscopic multiphonon basis

D. Bianco, F. Knapp,* N. Lo Iudice, F. Andreozzi, and A. Porrino
Dipartimento di Scienze Fisiche, Universitá di Napoli Federico II and Istituto Nazionale di Fisica Nucleare, Monte S. Angelo, via Cintia, I-80126 Napoli, Italy
(Received 27 October 2011; published 17 January 2012)

An equation of motion method for solving the nuclear eigenvalue problem in a basis of microscopic multiphonon states is reformulated consistently in terms of Tamm-Dancoff phonons. The potential and limits of the method are illustrated through the calculation of the nuclear response to dipole and quadrupole external fields in ^{16}O. The calculation is performed using either a Nilsson or a Hartree-Fock basis. The role of the multiphonon states is shown to depend strongly on the choice of the basis. The effect of the truncation of the three-phonon subspace is also discussed.

DOI: 10.1103/PhysRevC.85.014313 PACS number(s): 21.60.Ev, 21.10.Re, 24.30.Cz

I. INTRODUCTION

Extensions of the random-phase approximation (RPA) are needed in order to account for the fragmentation of the nuclear giant resonances [1] and to describe the anharmonic features of the multiphonon levels whose evidence is growing at low [2,3] and high [4] energy.

These extensions, known as second RPA (SRPA) [5,6], couple the particle-hole (ph) or quasiparticle (qp) RPA modes to the 2p2h or 4qp configurations.

The SRPA equations were solved in several approximations. The most drastic one was to neglect the mutual coupling among 2p2h states [7,8]. Another consisted in replacing one ph pair with a correlated state (RPA phonon) thereby obtaining a particle-phonon coupling [9–12]. A recent calculation using a Skyrme force takes into partial account the interaction between 2p2h states [13,14].

On equivalent approximations relies the relativistic RPA (RRPA) plus phonon coupling [15,16], based on Green function techniques originally developed within a nonrelativistic frame [17]. An upgraded version, dubbed relativistic quasiparticle time blocking approximation (RQTBA) [18,19], exploits updated techniques of the Landau-Migdal theory [20,21] to treat consistently the quasiparticle-phonon coupling.

All the above approaches include up to two ph or qp phonons. A selected set of qp RPA three-phonon states is taken into consideration only in the quasiparticle phonon model (QPM) [22]. This approach adopts a two-body Hamiltonian of separable form, which simplifies enormously the eigenvalue equations.

The SRPA and its relativistic variants as well as the QPM have become precious tools for investigating the fine structure of nuclear resonances. In particular they were used to analyze the properties of the dipole excitations observed in the low-energy queue of the giant dipole resonance (GDR), in nuclei with neutron excess. These excitations are associated to the pygmy dipole resonance (PDR), promoted by the oscillation of the neutron skin against the core. A rather complete and updated list of references on this subject may be found in Ref. [23].

Recently, we developed an equation of motion phonon method (EMPM) [24,25] which generates iteratively a multiphonon basis built of phonons obtained in ph Tamm-Dancoff approximation (TDA) and solves the eigenvalue problem in such a basis.

The formulation, however, was not entirely consistent. The n-phonon basis states, in fact, were obtained by acting with ph operators on the $(n-1)$-phonon states. Thus, eigenvalue equations, states and observables were expressed partly in terms of ph states and partly in terms of phonons. Such a hybrid structure inhibited the possibility of taking advantage of the phonon composition of the states to operate reliable truncations of the full space. We were thus forced to perform calculations in a rather restricted shell model space.

This inconsistency is removed in this new scheme where the ph operators are replaced by TDA phonons in the construction of each n-phonon basis state. In virtue of this simple change, the eigenvalue equations yield, with the same accuracy of shell model, states and observables expressed consistently and solely in terms of phonons.

With respect to the old formulation, this new version results to be more elegant and flexible. It enables us, for instance, to truncate the multiphonon space while taking high energy configurations into account. Indeed, the final goal of the phonon scheme is to achieve a maximal space truncation by selecting only the relevant phonons.

The eigenvalue problem is formulated first in the spin uncoupled basis and, then, in the $j-j$ coupled scheme. The first formulation provides equations of simple and physically transparent structure. The second, which results to be only slightly more involved, is more suited for numerical applications.

The method is applied to the doubly magic ^{16}O. We construct and solve the eigenvalue equations and use the eigenstates to study the dipole and quadrupole responses. The calculation is performed using either a Nilsson or a Hartree-Fock (HF) single particle basis within a space which includes the full two-phonon subspace and an appreciable fraction of three-phonon states.

*Permanent address: Faculty of Mathematics and Physics, Charles University in Prague, Czech Republic.

Such a numerical implementation is meant to clarify the relevance of the different phonon subspaces to the nuclear response, to test if and how their role depends on the single particle basis, and, finally, to explore to what extent a truncation of the three-phonon subspace affects spectra and transitions.

II. THE METHOD

As in Refs. [24,25], we write a two-body Hamiltonian H of general form in the second quantized form

$$H = \sum_i \epsilon_i a_i^\dagger a_i + \frac{1}{4}\sum_{ijkl} V_{ijkl}\, a_i^\dagger a_j^\dagger a_l a_k\,, \tag{1}$$

where ϵ_i are the single-particle energies, $a_i^\dagger$ (a_i) the creation (annihilation) particle operators with respect to the physical vacuum, and $V_{ijkl} = \langle ij|V|kl\rangle_A$ are antisymmetrized matrix elements of the nucleon-nucleon interaction.

A. Tamm-Dancoff approximation

The preliminary step consists in solving the TDA eigenvalue problem

$$\sum_{p'h'} A_{ph;p'h'} c^\lambda_{p'h'} = E_\lambda c^\lambda_{ph}, \tag{2}$$

where

$$A_{ph;p'h'} = \delta_{hh'}\delta_{pp'}(\epsilon_p - \epsilon_h) + V_{p\bar{h}'\bar{h}p'} \tag{3}$$

and $\bar{h}$ denotes time reversal. The solution of the TDA equations allows to construct the phonon operator

$$O^\dagger_\lambda = \sum_{ph} c^\lambda_{ph} a^\dagger_p a_{\bar{h}}\,, \tag{4}$$

where $a^\dagger_p$ ($a_{\bar{h}}$) creates a particle (hole) out of the unperturbed ground state $|0\rangle$, the ph vacuum.

The transition amplitudes of the one-body operator

$$\mathcal{M}_\lambda = \sum_{rs}\langle r|\mathcal{M}_\lambda|s\rangle a^\dagger_r a_s \tag{5}$$

are

$$\langle\lambda|\mathcal{M}_\lambda|0\rangle = \sum_{ph} c^{(\lambda)}_{ph}\langle p|\mathcal{M}_\lambda|\bar{h}\rangle. \tag{6}$$

An important quantity is the TDA density matrix:

$$\rho_{\lambda\lambda'}(rs) = \langle\lambda'|a^\dagger_r a_s|\lambda\rangle = \sum_k c^{(\lambda')}_{rk} c^{(\lambda)}_{sk}, \tag{7}$$

where $k = p$ or h according that $(rs) = (h_1h_2)$ or $(rs) = (p_1p_2)$, respectively. In the above formula $a^\dagger_r a_s$ are considered in normal order. Thus the contribution from the core is neglected.

B. Equations of motion and multiphonon basis

Our goal is to construct n-phonon states $|n;\beta\rangle$ so composed

$$|n;\beta\rangle = \sum_{\lambda\alpha} C^{(\beta)}_{\lambda\alpha}\, O^\dagger_\lambda\, |n-1;\alpha\rangle. \tag{8}$$

It is to be noticed the change with respect to the previous version [24,25], where the basis states were constructed out of $a^\dagger_p a_{\bar{h}}|n-1;\alpha\rangle$.

The procedure starts with writing the equations of motion

$$\langle n,\beta|[H, O^\dagger_\lambda]|n-1,\alpha\rangle = (E_\beta - E_\alpha)X^{(\beta)}_{\lambda\alpha}, \tag{9}$$

where

$$X^{(\beta)}_{\lambda\alpha} = \langle n,\beta|O^\dagger_\lambda|n-1,\alpha\rangle. \tag{10}$$

The above amplitudes are related to the expansion coefficients $C^{(\beta)}_{\lambda\alpha}$ of the states $|n;\beta\rangle$ [Eq. (8)] by

$$X^{(\beta)}_{\lambda\alpha} = \sum_{\lambda'\alpha'} \mathcal{D}_{\lambda\alpha,\lambda'\alpha'} C^{(\beta)}_{\lambda'\alpha'}, \tag{11}$$

where

$$\mathcal{D}_{\lambda\alpha,\lambda'\alpha'} = \langle n-1,\alpha'|O_{\lambda'}O^\dagger_\lambda|n-1,\alpha\rangle \tag{12}$$

is the metric matrix.

We now expand the commutator and follow exactly the procedure of Refs. [24,25] to obtain

$$\sum_{\gamma php'h'} c^\lambda_{ph} A_{\alpha\gamma}(ph;p'h')\langle n;\beta|a^\dagger_{p'}a_{\bar{h}'}|n-1;\gamma\rangle = E_\beta X^{(\beta)}_{\lambda\alpha}, \tag{13}$$

where

$$\begin{aligned}\mathcal{A}_{\alpha\gamma}&(ph;p'h')\\ &= \delta^{(n)}_{\alpha\gamma}\left[\delta_{hh'}\delta_{pp'}\left(\epsilon_p - \epsilon_h + E^{(n-1)}_\alpha\right) + V_{p\bar{h}'\bar{h}p'}\right]\\ &\quad + \sum_{h_1h_2}\left[\delta_{hh'}\,V_{p'h_1ph_2} - \delta_{pp'}\,\frac{1}{2}V_{hh_1h'h_2}\right]\rho^{(n-1)}_{\alpha\gamma}(h_1h_2)\\ &\quad + \sum_{p_1p_2}\left[\frac{1}{2}\delta_{hh'}\,V_{p'p_1pp_2} - \delta_{pp'}\,V_{hp_1h'p_2}\right]\rho^{(n-1)}_{\alpha\gamma}(p_1p_2).\end{aligned} \tag{14}$$

The quantities

$$\rho^{(n)}_{\alpha\gamma}(rs) \equiv \langle n;\gamma|a^\dagger_r a_s|n;\alpha\rangle \tag{15}$$

with $(rs) = (pp')$ or $(rs) = (hh')$ are the one-body density matrices in the n-phonon subspace. The matrix $\mathcal{A}$ contains the TDA matrix A given by Eq. (3). It actually turns into A for $n = 1$.

We now invert Eq. (4) to express the ph in terms of the phonon operators $O^\dagger_\lambda$ and obtain

$$\langle n;\beta|a^\dagger_p a_{\bar{h}}|n-1;\gamma\rangle = \sum_\lambda c^\lambda_{ph}\langle n,\beta|O^\dagger_\lambda|n-1,\gamma\rangle. \tag{16}$$

Once this quantity is inserted into Eq. (13), we observe that the coefficients c^λ_{ph} bring the TDA matrix contained in $\mathcal{A}_{\alpha\gamma}$ to diagonal form

$$\sum_{php'h'} c^\lambda_{ph} A(ph,p'h') c^{\lambda'}_{p'h'} = \delta_{\lambda\lambda'}E_\lambda. \tag{17}$$

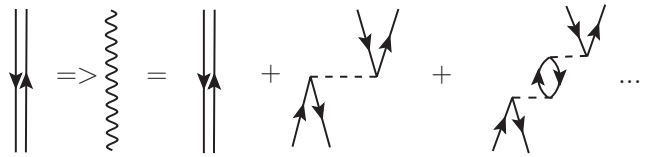

FIG. 1. From particle-hole to phonon propagators.

In virtue of this property, Eq. (13) becomes

$$\sum_{\lambda'\alpha'} \mathcal{A}_{\lambda\alpha,\lambda'\alpha'} X^{\beta}_{\lambda'\alpha'} = E_\beta X^{\beta}_{\lambda\alpha}, \tag{18}$$

where the matrix $\mathcal{A}$ is expressed solely in terms of phonons

$$\mathcal{A}_{\lambda\alpha,\lambda'\alpha'} = (E_\lambda + E_\alpha)\delta_{\lambda\lambda'}\delta_{\alpha\alpha'} + \mathcal{V}_{\lambda\alpha,\lambda'\alpha'}. \tag{19}$$

Here, E_λ and E_α are, respectively, the one- and $(n-1)$-phonon energies and $\mathcal{V}$ the phonon-phonon potential of the form

$$\mathcal{V}_{\lambda\alpha,\lambda'\alpha'} = \sum_{rs} \mathcal{V}_{\lambda\lambda'}(rs)\rho^{(n)}_{\alpha\alpha'}(rs), \tag{20}$$

where

$$\mathcal{V}_{\lambda\lambda'}(rs) = \sum_{tq} V_{trqs}\rho_{\lambda\lambda'}(qt). \tag{21}$$

The attention should be focused on the formal analogy of the structure (19) of the phonon matrix $\mathcal{A}_{\lambda\alpha,\lambda'\alpha'}$ with the form (3) of the TDA matrix $A_{ph;p'h'}$. Formally, the first is deduced from the second by replacing the particle-hole energies with the sum of phonon energies and the particle-hole interaction with a phonon-phonon interaction.

This correspondence can be illustrated in terms of diagrams. The TDA ph lines are replaced by phonons (Fig. 1) and each TDA ph vertex is turned into a phonon-phonon vertex (Fig. 2) which amounts to a sum of infinite diagrams in the two-body potential.

Unlike the case of TDA, however, Eq. (18) is not yet an eigenvalue equation. This is obtained once we express the X amplitudes in terms of the expansion coefficients C defined by Eq. (8). Equation (18) is thus turned into the generalized eigenvalue equation within the n-phonon space

$$\mathcal{H}C = (\mathcal{A}\mathcal{D})C = EC \tag{22}$$

or, more explicitly,

$$\sum_{\lambda'\alpha'} \mathcal{H}(\lambda\alpha,\lambda'\alpha')C^{\beta}_{\lambda'\alpha'} = \sum_{\lambda'\alpha'} (A\mathcal{D})(\lambda\alpha,\lambda'\alpha')C^{\beta}_{\lambda'\alpha'} = E_\beta \sum_{\lambda'\alpha'} \mathcal{D}_{\lambda\alpha,\lambda'\alpha'} C^{\beta}_{\lambda'\alpha'}. \tag{23}$$

The metric matrix can be shown to have the following expression:

$$\mathcal{D}_{\lambda\alpha,\lambda'\alpha'} = \delta_{\lambda\lambda'}\delta_{\alpha\alpha'} + \sum_{\gamma} X^{(\alpha)}_{\lambda'\gamma} X^{(\alpha')}_{\lambda\gamma} - \sum_{rs} \rho_{\lambda\lambda'}(rs)\rho^{(n-1)}_{\alpha\alpha'}(rs). \tag{24}$$

The corrective terms to unity are induced by the redundancy of the $O^{\dagger}_{\lambda}|n-1;\alpha\rangle$ states and enforce the Pauli principle.

The one-body densities in the n-phonon subspaces ($n > 1$) are given by

$$\rho^{(n)}_{\alpha\alpha'}(rs) = \langle n,\alpha'|a^{\dagger}_r a_s|n,\alpha\rangle = \sum_{\gamma\delta\lambda\lambda'} C^{(\alpha)}_{\lambda\gamma} X^{(\alpha')}_{\lambda'\delta}\left[\delta_{\gamma\delta}\rho_{\lambda\lambda'}(rs) + \delta_{\lambda\lambda'}\rho^{(n-1)}_{\gamma\delta}(rs)\right]. \tag{25}$$

Since recursive formulas hold for all quantities, the eigenvalue Eq. (23) can be solved iteratively once the TDA phonons are generated.

The redundant states are eliminated by the procedure outlined in Refs. [24,25], based on the Cholesky decomposition method. This method selects a basis of linear independent states $O^{\dagger}_{\lambda}|n-1;\alpha\rangle$ spanning the physical subspace of the correct dimensions $N_n < N_r$ and, thus, enables us to construct a $N_n \times N_n$ nonsingular matrix $\mathcal{D}_n$. By the left multiplication in the N_n-dimensional subspace we get from Eq. (22)

$$\left[\mathcal{D}_n^{-1}(\mathcal{A}\mathcal{D})\right]C = EC. \tag{26}$$

This equation determines only the coefficients $C^{(\beta)}_{\lambda\alpha}$ of the N_n-dimensional physical subspace. The remaining redundant $N_r - N_n$ coefficients are undetermined and, therefore, can be safely put equal to zero. The eigenvalue problem is thereby solved exactly. A set of orthonormal multiphonon states $\{|0\rangle, |1,\lambda\rangle, \ldots |n,\alpha\rangle \ldots\}$ is thus generated.

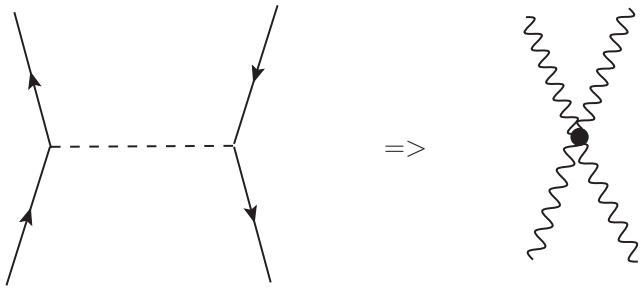

FIG. 2. From particle-hole to phonon-phonon interaction.

C. Eigenvalue problem in the multiphonon basis

The Hamiltonian is diagonal within each n-phonon subspace. For its complete diagonalization it is necessary to compute the nondiagonal pieces $\langle n',\beta|H|n,\alpha\rangle$. The only nonvanishing terms are those connecting states differing by one or two phonons. They are given by

$$\langle n;\beta|\, H\, |n-1;\alpha\rangle = \sum_{\lambda\gamma} \mathcal{V}_{\alpha\gamma}(\lambda) X^{(\beta)}_{\lambda\gamma}, \tag{27}$$

$$\langle n;\beta|H|n-2;\alpha\rangle = \sum_{\lambda\lambda'\gamma} \mathcal{V}_{\lambda\lambda'} X^{\beta}_{\lambda\gamma} X^{\gamma}_{\lambda'\alpha}, \tag{28}$$

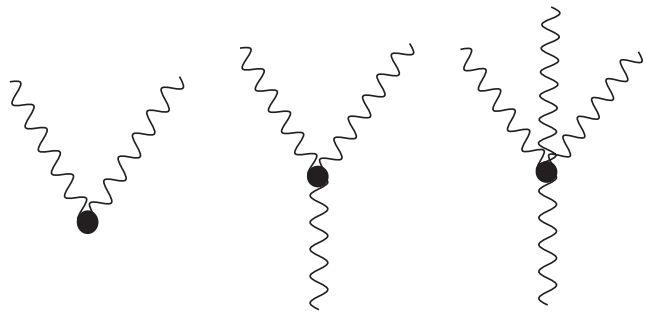

FIG. 3. Phonon coupling vertices.

where

$$\mathcal{V}_{\alpha\gamma}(\lambda) = \frac{1}{2}\sum_{rstq} c^{(\lambda)}_{tq} V^{(\lambda)}_{rtsq} \rho^{(n-1)}_{\alpha\gamma}(rs), \tag{29}$$

$$\mathcal{V}(\lambda\lambda') = \frac{1}{4}\sum_{rstq} V_{rtsq} c^{\lambda}_{rs} c^{\lambda'}_{tq}. \tag{30}$$

The above coupling terms may be represented diagrammatically as in Fig. 3.

The resulting Hamiltonian can be easily brought to diagonal form and yields eigenfunctions having the structure

$$|\Psi_\nu\rangle = \sum_{n\alpha} C^{(\nu)}_{\alpha} |n;\alpha\rangle. \tag{31}$$

The above formula holds also for the ground state which, therefore, is explicitly correlated. For instance, as shown in Fig. 4, the vertex coupling the $n = 0$ to the $n = 2$ phonon states amounts to a sum of an infinite series of diagrams promoting a highly correlated ground state. Indeed, our multiphonon eigenvalue problem is equivalent to shell model and extends RPA without having to rely on the quasiboson approximation.

D. Transition amplitudes of one-body operators

Using the above wave functions we can compute the transition amplitudes of the one-body operator $\mathcal{M}_\lambda$, given by

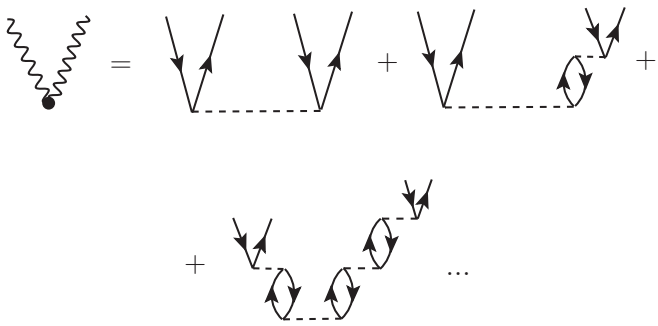

FIG. 4. Phonon vertex responsible for the ground state correlations.

Eq. (5), obtaining the expressions

$$\mathcal{M}_\lambda(i \to f) = \langle \Psi_{\nu_f} | \mathcal{M}_\lambda | \Psi_{\nu_i} \rangle = \sum_{\beta_i\beta_f} C^{(\nu_i)}_{\beta_i} C^{(\nu_f)}_{\beta_f} \langle n_f, \beta_f | \mathcal{M}_\lambda | n_i, \alpha_i \rangle, \tag{32}$$

where

$$\begin{aligned}\langle n_f, \beta_f | \mathcal{M}_\lambda | n_i, \beta_i \rangle &= \delta_{n_f n_i} \sum_{rs} \langle s | \mathcal{M}_\lambda | r \rangle \rho^{(n_i)}_{\beta_i\beta_f}(rs) \\ &+ \delta_{n_f(n_i-1)} \sum_{x} \langle x\lambda | \mathcal{M}(\lambda) | 0 \rangle X^{(\beta_f)}_{(x\lambda)\beta_i} \\ &+ \delta_{n_f(n_i+1)} \sum_{x} \langle x\lambda | \mathcal{M}(\lambda) | 0 \rangle X^{(\beta_i)}_{(x\lambda)\beta_f}.\end{aligned} \tag{33}$$

The first is a scattering term where states with the same number of phonons are coupled though the single-particle transition matrix elements, $\langle s|M_\lambda|r\rangle$, weighted by the particle or hole density matrices. The other two terms contain the TDA transition amplitudes $\langle x\lambda|\mathcal{M}(\lambda)|0\rangle$ given by Eq. (6). The label x distinguishes the TDA states with the same quantum numbers λ. These two terms are responsible for the coupling between multiphonon components differing by one phonon.

III. EMPM IN THE COUPLED SCHEME

The eigenvalue equations keep a simple structure even in the coupled $j - j$ scheme. The two pieces of the Hamiltonian

$$H = H_0 + V \tag{34}$$

assume the form

$$H_0 = \sum_r [r]^{1/2} \epsilon_r (a^\dagger_r \times b_r)^0, \tag{35}$$

$$V = -\frac{1}{4}\sum_{ijkl}^{\Gamma} [\Gamma]^{1/2} V^{\Gamma}_{rsqt} [(a^\dagger_r \times a^\dagger_s)^\Gamma \times (b_q \times b_t)^\Gamma]^0, \tag{36}$$

where

$$V^{\Gamma}_{rsqt} = \langle (q \times t)^\Gamma | V | (r \times s)^\Gamma \rangle - (-)^{r+s-\Gamma} \langle (q \times t)^\Gamma | V | (s \times r)^\Gamma \rangle. \tag{37}$$

Following French notation [26], we have put $b_r = (-)^{j_r+m_r} a_{j_r-m_r}$ and $[\Gamma] = 2\Gamma + 1 = (2J_\Gamma + 1)$.

It is useful to write the two-body potential (36) in the recoupled form

$$V = \frac{1}{4}\sum_{rsqt\sigma} [\sigma]^{1/2} F^{\sigma}_{rsqt} [(a^\dagger_r \times b_s)^\sigma \times (a^\dagger_q \times b_t)^\sigma]^0, \tag{38}$$

where

$$F^{\sigma}_{rsqt} = \sum_{\Gamma} [\Gamma](-)^{r+t-\sigma-\Gamma} W(rsqt;\sigma\Gamma) V^{\Gamma}_{rqst} \tag{39}$$

and $W(rsqt;\sigma\Gamma)$ are Racah coefficients.

The states to be generated in the $j - j$ coupled scheme must have the structure

$$|n;\beta\rangle = \sum_{\lambda\alpha} C^{(\beta)}_{\lambda\alpha} \{O^\dagger_\lambda \times |n-1,\alpha\rangle\}^\beta. \tag{40}$$

To this purpose, we start with the equations of motion

$$\langle n,\beta|\{[H,O^\dagger_\lambda]\times|n-1,\alpha\rangle\}^\beta = (E_\beta - E_\alpha)\langle n,\beta|\{O^\dagger_\lambda\times|n-1,\alpha\rangle\}^\beta. \quad (41)$$

Using the Wigner Eckart theorem we get

$$\langle n,\beta\|[H,O^\dagger_\lambda]\|n-1,\alpha\rangle = (E_\beta - E_\alpha)\langle n,\beta\|O^\dagger_\lambda\|n-1,\alpha\rangle. \quad (42)$$

We now expand the commutator and follow the same procedure as in the uncoupled case. The derivation is, of course, more involved since one has to make a massive use of Racah algebra. The outcome of this series of operations is

$$\sum_{\lambda'\gamma} A(\lambda\alpha,\lambda'\gamma)X^\beta_{\lambda'\gamma} = E_\beta X^\beta_{\lambda\alpha}, \quad (43)$$

where

$$X^\beta_{\lambda\alpha} = \langle n,\beta\|O^\dagger_\lambda\|n-1,\alpha\rangle. \quad (44)$$

Expanding $X^\beta_{\lambda\alpha}$ in terms of the coefficients $C^\beta_{\lambda\alpha}$, defined by Eq. (40), we obtain the generalized eigenvalue equation

$$\sum_{\lambda'\gamma\lambda''\gamma'} \mathcal{A}_{\lambda\alpha,\lambda'\gamma}\mathcal{D}^\beta_{\lambda'\gamma,\lambda''\gamma'}C^\beta_{\lambda''\gamma'} = E_\beta \sum_{\lambda'\gamma}\mathcal{D}^\beta_{\lambda\alpha,\lambda'\gamma}C^\beta_{\lambda'\gamma}. \quad (45)$$

The matrix $\mathcal{A}$ has the simple structure

$$\mathcal{A}_{\lambda\alpha,\lambda'\gamma} = (E_\lambda + E_\alpha)\delta_{\lambda\lambda'}\delta_{\alpha\gamma} + \sum_\sigma W(\beta\lambda'\alpha\sigma;\gamma\lambda)\mathcal{V}^\sigma_{\lambda\alpha,\lambda'\gamma}. \quad (46)$$

The phonon-phonon potential is given by

$$\mathcal{V}^\sigma_{\lambda\alpha,\lambda'\gamma} = \sum_{rs}^{(\pi)}\mathcal{V}^\sigma_{\lambda\lambda'}(rs)\rho^{(n)}_{\alpha\gamma}([r\times s]^\sigma), \quad (47)$$

where

$$\mathcal{V}^\sigma_{\lambda\lambda'}(rs) = \sum_{tq}\rho_{\lambda\lambda'}([q\times t]^\sigma)F^\sigma_{qtrs}. \quad (48)$$

The metric matrix is given by

$$\mathcal{D}^{(\beta)}(\alpha\lambda;\alpha'\lambda') = [\langle n-1,\alpha'|\times O_{\lambda'}]_\beta[O^\dagger_\lambda\times|n-1'\alpha\rangle]_\beta = \delta_{\lambda\lambda'}\delta_{\alpha\alpha'} + \sum_\gamma W(\alpha'\lambda\lambda'\alpha;\gamma\beta)X^\alpha_{\gamma\lambda'}X^{\alpha'}_{\gamma\lambda} + (-)^{\alpha+\beta+\lambda}\sum_\sigma W(\lambda'\lambda\alpha'\alpha;\sigma\beta)R_{\lambda\alpha,\lambda'\alpha'}, \quad (49)$$

having put

$$R_{\lambda\alpha,\lambda'\alpha'} = \sum_{rs}\rho_{\lambda\lambda'}([r\times s]^\sigma)\rho^{(n-1)}_{\alpha\alpha'}([r\times s]^\sigma). \quad (50)$$

The TDA density matrix has the expression

$$\rho_{\lambda\lambda'}([r\times s]^\sigma) = \langle\lambda'\|(a^\dagger_r\times b_s)^\sigma\|\lambda\rangle = [\lambda\lambda'\sigma]^{1/2}\sum_t c^\lambda_{ts}\,c^{\lambda'}_{tr}W(\lambda' t\sigma s;r\lambda), \quad (51)$$

where it is meant that $t = p$ when $(rs) = (hh')$ and $t = h$ when $(rs) = (pp')$.

For the n-phonon density matrix we obtain

$$\rho^{(n)}_{\alpha\alpha'}([r\times s]^\sigma) = \langle n;\alpha'\|[a^\dagger_r\times b_s]^\sigma\|n;\alpha\rangle = \sum_{\lambda\lambda'}\rho_{\lambda\lambda'}([r\times s]^\sigma)Y^\sigma_{\lambda\lambda'}(\alpha\alpha') + \sum_{\gamma\gamma'}\rho^{(n-1)}_{\gamma\gamma'}([r\times s]^\sigma)Y^\sigma_{\gamma\gamma'}(\alpha\alpha'), \quad (52)$$

where

$$Y^\sigma_{\lambda\lambda'}(\alpha\alpha') = [\alpha]^{1/2}\sum_\gamma W(\alpha'\sigma\gamma\lambda;\alpha\lambda')C^\alpha_{\lambda\gamma}\,X^{\alpha'}_{\lambda'\gamma},$$
$$Y^\sigma_{\gamma\gamma'}(\alpha\alpha') = [\alpha]^{1/2}\sum_\lambda(-)^{\alpha-\alpha'+\gamma-\gamma'} \times W(\alpha'\sigma\lambda\gamma;\alpha\gamma')C^\alpha_{\lambda\gamma}\,X^{\alpha'}_{\lambda\gamma'}. \quad (53)$$

Having constructed the generalized eigenvalue Eq. (45), we can generate a basis of multiphonon states by following the procedure outlined in Sec. II B for the uncoupled scheme, based on the Cholesky decomposition method.

It remains, therefore, to derive and compute the nondiagonal terms. For the states differing by one phonon we get

$$\langle n,\beta|H|n-1,\alpha\rangle = [\beta]^{-1}\sum_{\sigma\gamma}\mathcal{V}^\sigma_{\alpha\gamma}X^{(\beta)}_{\sigma\gamma}, \quad (54)$$

where

$$\mathcal{V}^\sigma_{\alpha\gamma} = (-)^{\alpha+\gamma+\sigma}\sum_{rs}\mathcal{V}^\sigma_{rs}\rho^{(n-1)}_{\alpha\gamma}([r\times s]^\sigma) \quad (55)$$

and

$$\mathcal{V}^\sigma_{rs} = \frac{1}{2}\sum_{ph}c^\sigma_{ph}F^\sigma_{phrs}. \quad (56)$$

The matrix elements of H between states differing by two phonons are given by

$$\langle n,\beta|H|n-2,\alpha\rangle = [\beta]^{-1}(-)^{\beta+\gamma}\sum_{(ik)\sigma}^{\gamma}(-)^\sigma X^\beta_{(i\sigma)\gamma}X^\gamma_{(k\sigma)\alpha}\mathcal{V}^\sigma_{ik}, \quad (57)$$

where i and k label the states with the same angular momentum σ and

$$\mathcal{V}^\sigma_{ik} = \frac{1}{4}\sum_{php_1h_1}F^\sigma_{php_1h_1}c^{i\sigma}_{ph}c^{k\sigma}_{p_1h_1}. \quad (58)$$

The multiphonon Hamiltonian matrix can now be brought to diagonal form. The resulting eigenstates may be used to compute the transition amplitudes.

In the coupled scheme, the one-body operator has the form

$$\mathcal{M}_{\lambda\mu} = \frac{1}{[\lambda]^{1/2}}\sum_{rs}\langle r\|\mathcal{M}_\lambda\|s\rangle[a^\dagger_r\times a_s]_{\lambda\mu}. \quad (59)$$

The reduced transition amplitudes are given by

$$\langle\Psi_{\nu_f J_f}\|\mathcal{M}_\lambda\|\Psi_{\nu_i J_i}\rangle = \sum_{\beta_i\beta_f}C^{(\nu_i)}_{\beta_i}C^{(\nu_f)}_{\beta_f}\langle n_f,\beta_f J_f\|\mathcal{M}_\lambda\|n_i,\alpha_i J_i\rangle, \quad (60)$$

where the matrix elements of $\mathcal{M}_\lambda$ between multiphonon states are

$$\begin{aligned}\langle n_f;\beta_f J_f\|\mathcal{M}_\lambda\|n_i;\beta_i J_i\rangle &= [\lambda]^{-1/2}\Bigg[\delta_{n_f n_i}\sum_{rs}\langle r\|\mathcal{M}_\lambda\|s\rangle\rho^{(n_i)}_{\beta_i\beta_f}([r\times s]^\lambda)\\ &+\delta_{n_f(n_i+1)}\sum_x \mathcal{M}[0\to(x\lambda)]X^{(\beta_f)}_{x\lambda\beta_i}\\ &+\delta_{n_f(n_i-1)}\sum_x \mathcal{M}[0\to(x\lambda)](-)^{J_f-J_i+\lambda}X^{\beta_i}_{x\lambda\beta_f}\Bigg].\end{aligned}\tag{61}$$

Here

$$\mathcal{M}[0\to(x\lambda)]=\langle x\lambda\|\mathcal{M}_\lambda\|0\rangle=\sum_{ph}c^{(x\lambda)}_{ph}\langle p\|\mathcal{M}_\lambda\|h\rangle\tag{62}$$

are the TDA reduced transition amplitudes.

IV. NUMERICAL IMPLEMENTATION

The practical implementation starts with the following preliminary calculations:

(i) Solve the TDA eigenvalue equations (3) ($n=1$) and obtain the eigenvalues E_λ and the eigenstates $|\lambda\rangle$.
(ii) Use the expansion coefficients c^λ_{ph} of the TDA states $|\lambda\rangle$ to compute the matrix elements of the renormalized interaction $\mathcal{V}^\sigma_{\lambda\lambda'}(rs)$ given by Eq. (48) and the TDA density matrix $\rho_{\lambda\lambda'}([r\times s]^\sigma)$ given by Eq. (51).

The quantities E_λ, $\mathcal{V}^\sigma_{\lambda\lambda'}(rs)$ and $\rho_{\lambda\lambda'}([r\times s]^\sigma)$ are the entries for the iterative procedure which generates the multiphonon basis. This goes through the following steps:

For $n=2,3,\ldots$

(i) Compute the density matrix $\rho^{(n-1)}$ through Eq. (52).
(ii) Compute the metric matrix $\mathcal{D}$ through Eq. (49) using $\rho^{(n-1)}$ and $X(n-1)$.
(iii) Compute the matrix $\mathcal{A}$ [Eq. (46)] using E_λ and $\mathcal{V}$ as input and the just computed density matrices $\rho^{(n-1)}$.
(iv) Perform the Cholesky decomposition method to extract the linear independent $O^\dagger_\lambda|(n-1),\alpha\rangle$ states.
(v) Construct the inverse matrix $\mathcal{D}_n^{-1}$ and perform the matrix multiplication $\mathcal{D}_n^{-1}\mathcal{A}\mathcal{D}$.
(vi) Solve the generalized eigenvalue problem (26) for the n-phonon subspace.
(vii) Repeat the same procedure for $n'=n+1$ starting from step (i).

It must be stressed that no approximations are involved in the process of generating such a multiphonon basis. On the other hand, we have to pay a price for it. The number of redundant states increases very rapidly with the number of phonons. Though eliminated at the end of the process, they enter in the formulas defining the matrices $\mathcal{A}$ and $\mathcal{D}$. This redundancy has the effect of slowing down considerably the procedure if we keep all basis states.

Once generated, the multiphonon basis can be used to complete the construction of the Hamiltonian matrix by computing the nondiagonal matrix elements (54) and (57). We are finally able to solve the eigenvalue equations in the full multiphonon space obtaining the eigenvalues and eigenvectors of the nuclear Hamiltonian.

V. NUCLEAR RESPONSE TO EXTERNAL FIELDS IN ^{16}O

Our EMPM calculations were focused on the study of giant resonances in ^{16}O. A similar calculation was recently performed in SRPA [13] using a density dependent Skyrme potential, which accounts for the coupling between ph and 2p2h. Here, we included up to three phonons.

We used a Brueckner G matrix [27,28] derived from the CD-Bonn NN potential [29] and treated the Hamiltonian in both Nilsson and HF bases. For the Nilsson Hamiltonian we chose the parameters appropriate for $A=16$ [30]. The harmonic oscillator frequency was taken to be $\hbar\omega=41A^{-1/3}$ MeV. For the spin-orbit coupling constant $C=-2\hbar\omega\kappa$ we put $\kappa=0.12$, while we took a vanishing value for the l^2 term.

The configuration space covered up to the (p,f) shell. The number of states increases very rapidly as the configuration space is enlarged and/or the number of phonons increases. We kept all two-phonon states and performed a truncation of the three-phonon space by keeping all the states up to some energy value.

A. Removal of the center-of-mass motion

In computing the nuclear response it is important to get eigenstates free of center-of-mass spurious admixtures. As in Refs. [24,25], we followed the widely adopted prescription [31,32] of adding to the nuclear Hamiltonian H an harmonic oscillator Hamiltonian in the center-of-mass coordinates $\mathbf{R}$ and $\mathbf{P}$

$$H_g=g\left(\frac{P^2}{2Am}+\frac{1}{2}mA\omega^2R^2-\frac{3}{2}\hbar\omega\right),\tag{63}$$

where g is a multiplicative constant.

In the shell model, the center-of-mass spurious state can be completely eliminated as long as a pure harmonic oscillator basis is adopted and only and all configurations up to a given $N_{\max}$ major shell are included.

This condition was necessary also in the previous version of the EMPM due to the ph composition of the multiphonon states. Thus we were forced to include only the configurations up to $3\hbar\omega$.

This constraint is removed in the present phonon context. Indeed, we have first separated the TDA $J^\pi=1^-$ spurious phonons from the other TDA states. This separation is practically exact in the Nilsson basis and achieved with good approximation also in the HF basis no matter how large is the ph space. In fact, the center of mass Hamiltonian couples only the $J^\pi=1^-$ ph states of energy $1\hbar\omega$.

The phonon composition of the basis states guarantees that, for a sufficiently large constant g, the multiphonon states

containing the spurious TDA $J^\pi = 1^-$ are pushed up in energy and, finally, eliminated.

This prescription removes the necessity of considering only and all the shell model states up to a given $N_{\max}$ major shell and, therefore, allows us to include configurations of arbitrary excitation energy with obvious advantages. In our case, for instance, the energies of the multiphonon basis states range from $1\hbar\omega$ up to $9\hbar\omega$.

B. Strength function and cross section

The properties of giant resonances were investigated through the nuclear response to external probes. To this purpose it was useful to compute the strength functions

$$\mathcal{S}(E\lambda,\omega) = \sum_\nu B_\nu(E\lambda)\,\delta(\omega-\omega_\nu) \approx \sum_\nu B_\nu(E\lambda)\,\rho_\Delta(\omega-\omega_\nu), \quad (64)$$

where ω is the energy variable, ω_ν the energy of the transition of multipolarity $E\lambda$ from the ground to the ν_{th} excited state $\Psi_{\nu\lambda}$ of spin $J=\lambda$ and

$$\rho_\Delta(\omega-\omega_\nu) = \frac{\Delta}{2\pi}\frac{1}{(\omega-\omega_\nu)^2+\left(\frac{\Delta}{2}\right)^2} \quad (65)$$

is a Lorentzian of width Δ, which replaces the δ function as a weight of the reduced transition probability

$$B_\nu(E\lambda) = |\langle\Psi_{\nu\lambda}\|\mathcal{M}(E\lambda)\|\Psi_0\rangle|^2. \quad (66)$$

For all the $E\lambda$ transitions, we adopted the standard multipole operator

$$\mathcal{M}(E\lambda\mu) = \frac{e}{2}\sum_{i=1}^{A}(1-\tau_3^i)r_i^\lambda Y_{\lambda\mu}(\hat{r}_i), \quad (67)$$

where $\tau_3 = 1$ for neutrons and $\tau_3 = -1$ for protons.

For the giant dipole resonance, the cross section was also computed through the formula

$$\sigma_{\rm int} = \int_{E_0}^{E}\sigma(\omega)d\omega = \frac{16\pi^3e^2}{9\hbar c}\int_{E_0}^{E}\omega\mathcal{S}(E1,\omega)d\omega. \quad (68)$$

C. Results and discussion

As already mentioned, the space used for solving the eigenvalue equations covers the whole one- + two-phonon subspaces. The three-phonon states $O_\lambda^\dagger|n=2,\alpha\rangle$ included in the calculations were those obtained by coupling all one-phonons $O_\lambda^\dagger$ to the two-phonons $|n=2,\alpha\rangle$ of energy $E_\alpha \leqslant E_{\max}$. We chose $E_{\max} = 25$ MeV. The resulting eigenfunctions were used to compute the E_λ transition amplitudes.

Let us analyze first the $E1$ response. Figure 5 shows the strength function computed in the Nilsson (left) and HF (right) bases. In the Nilsson basis, the TDA strength is peaked around ~22 MeV, in agreement with experiments. The strength distribution does not undergo appreciable changes in going from the TDA to the multiphonon space.

The most visible effect is the ~16 MeV shift toward higher energies once the two-phonon space is added. The peaks are pushed down as the three-phonon states are included and tend to approach the TDA peaks if we increase the number of three-phonon states by raising the upper limit for the two-phonon energy from $E_{\max} = 25$ MeV to $E_{\max} = 30$ MeV. In order to reach eventually the region of the TDA peaks, as requested by the data, we should enlarge further the three-phonon subspace. This, however, would require too long computing time.

If a HF basis is adopted, the $E1$ response gets considerably damped and fragmented already at the TDA level, as shown in the right panels of Fig. 5. This result can be easily understood. One may conceive each Nilsson ph state as a linear combination of several HF ph components. Thus, the strength, which in the Nilsson basis is concentrated into a relatively short energy range, is redistributed over many more HF states spread over a much wider energy interval.

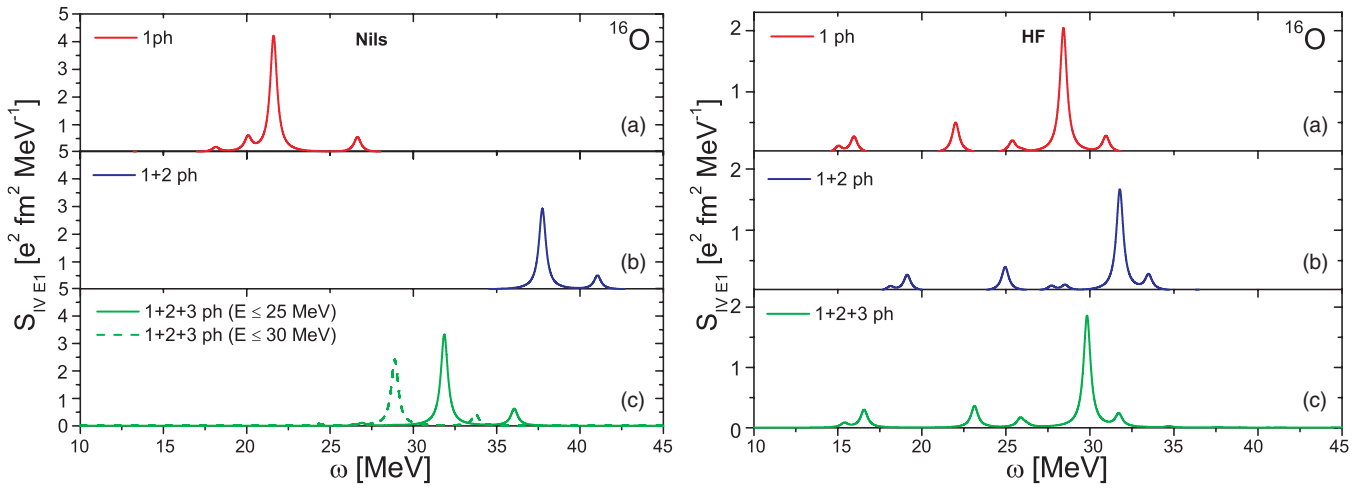

FIG. 5. (Color online) $E1$ strength function in a Nilsson (left) and a HF (right) basis in ^{16}O. (a), (b), and (c) show the response computed in the one-, (one + two)-, and (one + two + three)-phonon spaces, respectively.

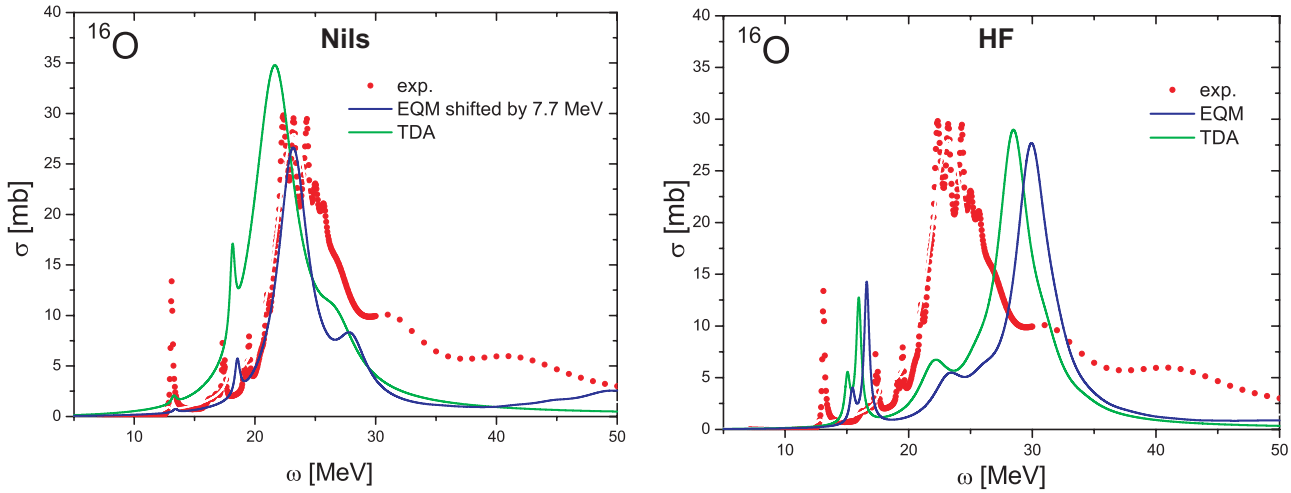

FIG. 6. (Color online) $E1$ cross section computed in a Nilsson (left) and a HF (right) basis in ^{16}O. The experimental data taken from Ref. [33] are shown for comparison.

The phonon coupling is much weaker than in the Nilsson basis. In fact, the two-phonon subspace pushes the peaks upward by ~ 5.5 MeV, while the three-phonon states bring the strength back to approximately the TDA energies. The net result is that the main peak is around $\sim$30 MeV, well above the experimental one.

The $E1$ cross section computed in the multiphonon space using the Nilsson basis is somewhat quenched with respect to TDA. As shown in Fig. 6 (left), it is in fair agreement with the experimental data [33], if the peaks are shifted down to the experimental region. This artificial shift is somewhat justified. It has been pointed out, in fact, that the computed strength approaches more and more the region of the main experimental peaks as an increasing number of three-phonon states is taken into consideration.

Of comparable quality is the agreement with the data of the $E1$ cross section computed in the HF basis [Fig. 6 (right)]. The cross section remains practically unchanged in going from TDA to the three-phonon space. The slight energy shift could be eliminated by increasing the number of three-phonon states.

Figure 7 shows the $E2$ strength function computed in the Nilsson (left) and HF (right) bases. As in the case of the dipole response, the isoscalar $E2$ strength, computed in the Nilsson basis, is shifted upward, though to a less extent ($\sim$12 MeV), when the TDA states are coupled to the two-phonon space. It is, then, pushed downward toward the TDA peak, once the three-phonon states are included. Whether computed in TDA or in the multiphonon space, the $E2$ spectrum is at too high energy with respect to the observed 2^+ levels.

Unlike the dipole response, the $E2$ strength gets strongly damped and fragmented once the two phonons are added. A further redistribution of the strength is induced by the three-phonon states.

The HF basis severely quenches and fragments the $E2$ strength already at the TDA level (right panels of Fig. 7). The role of the phonons is nonetheless important. The damping and fragmentation of the strength increase considerably as we add the two- and three-phonon spaces. The energy of the lowest 2^+ states is far above the experimental values, just as in the Nilsson case.

Let us try to understand why the multiphonon states play a very different role according that a Nilsson or a HF basis is adopted and why they have a different impact on the dipole and quadrupole responses.

Two factors play an important role, the energy scale of the multiphonon states and the hierarchy ruling the different phonon couplings.

According to this hierarchy, the spaces differing by two phonons are coupled by the Hamiltonian more strongly than those differing by one phonon. This implies that the ph vacuum $|0\rangle$ is strongly coupled to the $|n = 2, \alpha\rangle$ two-phonon states, the one-phonon states $|\lambda\rangle$ couple strongly to the three-phonon states $|n = 3, \alpha\rangle$ and so on.

It follows that the ground state Ψ_0 is strongly pushed down in energy by the coupling between the $|0\rangle$ vacuum and the two-phonon states. In the Nilsson basis, the shift amounts to $\Delta E = -20.8$ MeV.

The negative parity 1^- states are little affected by the two-phonon states. These, being built of a tensor product of negative parity $\sim 1\hbar\omega$ and positive parity $\sim 2\hbar\omega$ phonons, have unperturbed energies of the order $\sim 3\hbar\omega$. The weak one- to two-phonon coupling is not sufficient to admix them with the TDA 1^- phonons.

The three-phonon states, though having energies of the same order $\sim 3\hbar\omega$, are strongly coupled to the TDA phonons by the Hamiltonian. This coupling pushes the energies of the 1^- states downward and tends to counterbalance the shift of the ground state induced by the coupling between the vacuum and the two phonons.

In the case of the $E2$ response, one- and two-phonon components of the 2^+ states, having both energies of the order $\sim 2\hbar\omega$, get admixed, even though their mutual coupling is relatively weak. Hence, the much more pronounced fragmentation of the $E2$ strength with respect to the dipole response. The three-phonon components are at much higher energies, $\geqslant 4\hbar\omega$ and are less effective in pushing the 2^+ states down in energy through their coupling with the one-phonon components.

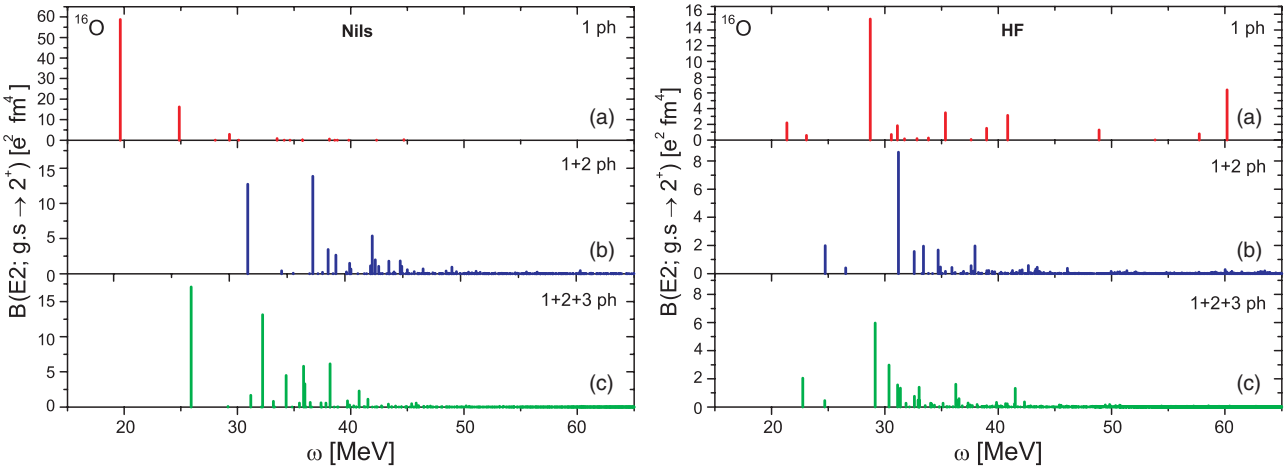

FIG. 7. (Color online) Isoscalar $E2$ reduced strength in a Nilsson (left) and a HF (right) basis in ^{16}O. (a), (b), and (c) show the response computed in the one-, (one + two)-, and (one + two + three)-phonon spaces, respectively.

The impact of phonons is much weaker in the HF basis, especially in the case of the $E1$ response. The HF states, indeed, admix the low-lying with the high-energy harmonic oscillator shells. These admixtures induce a large separation between the single particle energies and therefore shift the TDA phonons at higher energies. The single particle admixing has also the effect of weakening the phonon coupling. Such a coupling is rendered even less effective when the energy separation between states with different phonons is too high as in the 1^- states.

Even in HF, however, the effect of the multiphonon states is not negligible. Especially important is their contribution to the $E2$ response, given the comparable energy of one and two-phonon components. Appreciable is also the energy shift of the ground state, $\Delta E \sim -6$ MeV, induced by the coupling of the vacuum with the two-phonon states.

The role of the multiphonon components emerges also from the structure of the states. In the case of the Nilsson basis, the ground state Ψ_0 is characterized mainly by the ph vacuum with an appreciably large two-phonon component ($\sim$25%) [Fig. 8(a)]. One and three phonons are practically absent. This composition reflects the dominance of the coupling between the $|0\rangle$ vacuum and the two-phonon subspace.

An analogous structure is obtained for Ψ_0 in the HF basis [Fig. 8(b)]. The ground state correlations, however, get drastically reduced. The two-phonon components, in fact, account for $\sim$10%.

Figure 8 shows the occurrence at low energy of 0^+ states with a two-phonon dominance. The presence of states so composed is not surprising. One- and two-phonon states have comparable energies and get admixed.

The multiphonon states play an important role also in the 2^+ states, whose structure is similar to the one of the excited 0^+. In the Nilsson basis, several 2^+ are characterized by large two-phonon components, as is the case of the ones shown in Fig. 9(a). The same figure shows that the two-phonon components may be dominant in the 2^+ states also when the HF basis is adopted [Fig. 9(b)].

The above analysis offers a key for explaining why the lowest 2^+ (and 0^+) states are at too high energy compared to

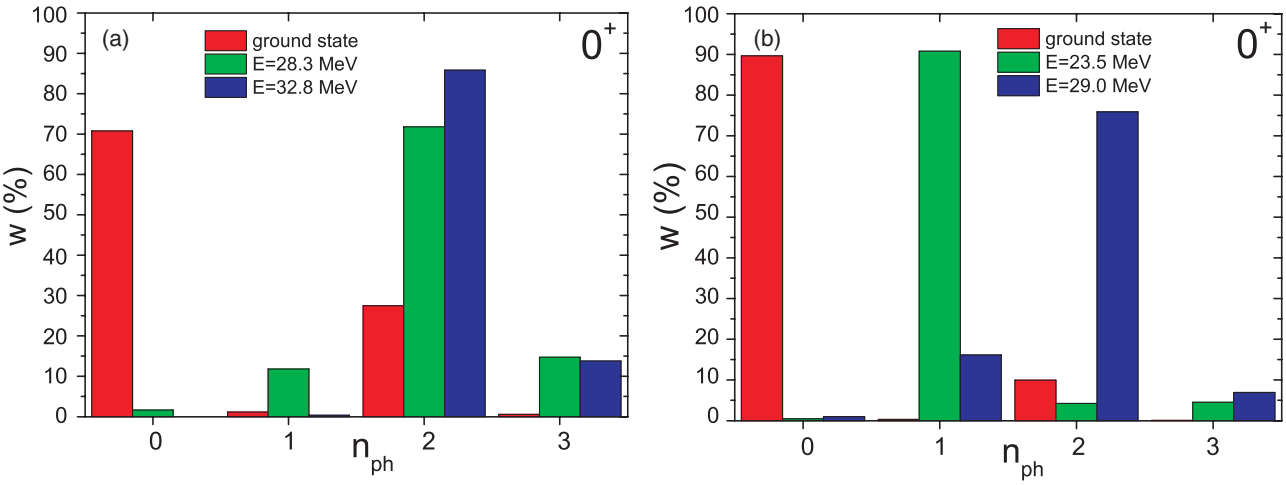

FIG. 8. (Color online) Phonon structure of some 0^+ states in a Nilsson (a) and a HF (b) basis in ^{16}O.

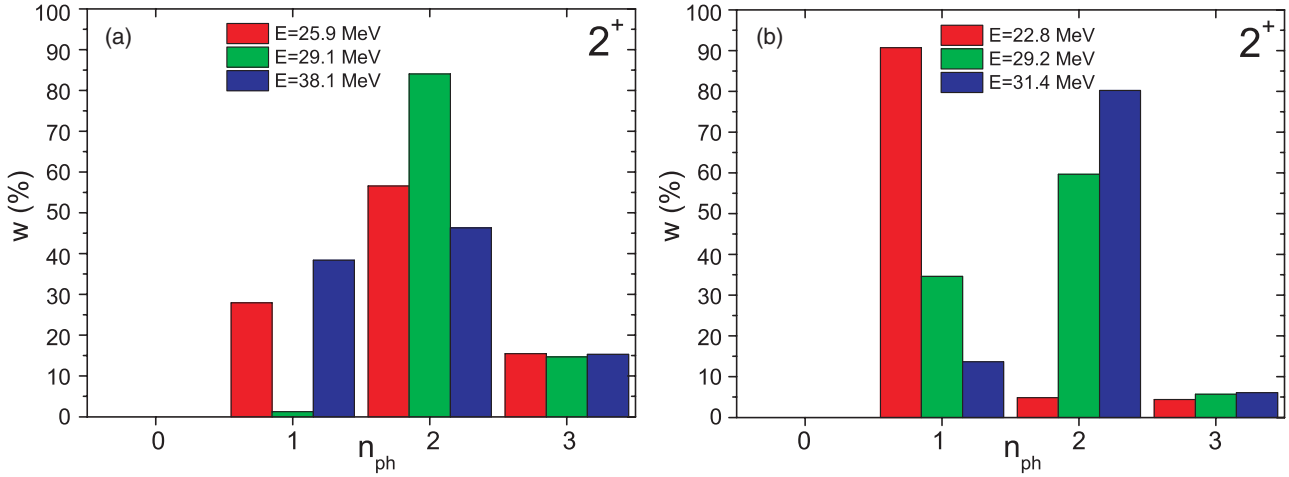

FIG. 9. (Color online) Phonon structure of some 2^+ states in a Nilsson (a) and a HF (b) basis in ^{16}O.

the experimental levels. Several 2^+, especially in the Nilsson, are dominantly two-phonon states and, therefore, are supposed to couple strongly to the four-phonon states which are at $\sim 4\hbar\omega$. Thus, in order to push down their energies toward the experimental values, we need to include the four-phonon subspace, at least. This is consistent with the results obtained in the large scale shell model calculations [34,35], where the states are classified according to their $N\hbar\omega$ excitations.

The first two 1^- states, including the one corresponding to the strongest peak, have a dominant one-phonon structure [Fig. 10(a)]. In the Nilsson basis, the three-phonon components account for about $\sim$15%, more than the two-phonon share. Both two- and three-phonon weights are quite small in the HF basis [Fig. 10(b)].

VI. CONCLUDING REMARKS

In this upgraded version of the method, the equations of motions generate multiphonon basis states consistently composed of TDA phonons, rather than particle-hole states. These equations have a very simple, physically transparent, structure. They are, in fact, the phonon analog of the ph TDA equations.

This consistent scheme is more flexible and allows to truncate the multiphonon space while accounting for high energy configurations incorporated in the TDA phonons.

The calculation of the nuclear response to dipole and quadrupole external fields in ^{16}O shows that the effect of the multiphonon states depends critically on the single particle basis adopted and differs strongly in going from the dipole to the quadrupole response.

In the Nilsson basis, the $E1$ resonance, while keeping its shape, is strongly pushed up in energy once the space is enlarged so as to include the two-phonon states and then shifted backward as we add the three phonons.

An analogous, though less strong, energy shift mechanism holds for the $E2$ transitions. Unlike the $E1$ response, the $E2$ strength gets strongly fragmented in going from TDA to the multiphonon space.

The energy shifts and the strength fragmentation result from a competition between the energies of the multiphonon states and their mutual coupling. This is weak or strong according

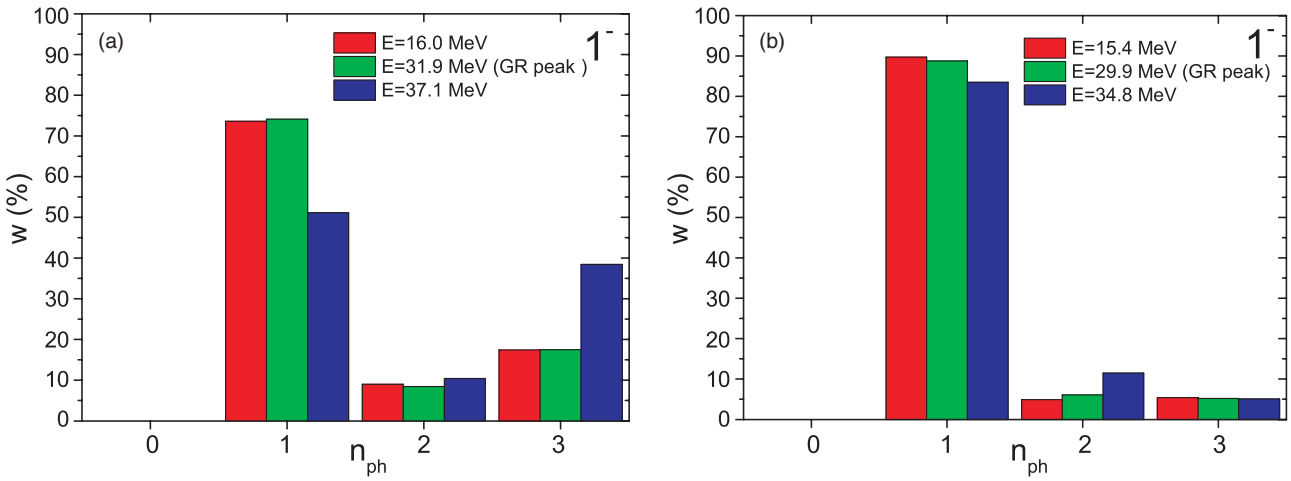

FIG. 10. (Color online) Phonon structure of some 1^- states in a Nilsson (a) and a HF (b) basis in ^{16}O.

that the coupled states differ by one or two phonons. In particular, the coupling of the ph vacuum with the two-phonon states induces strong correlations in the ground state and shifts downward its energy. This shift is ignored in most approaches due to their approximate treatment of the ground state correlations.

The role of phonons becomes less important if a HF basis is adopted. Such a basis induces a fragmentation of the strength, already at the TDA level, for both dipole and quadrupole responses and weakens drastically the phonon coupling. Thus, the energy shift of the strengths induced by such a coupling is more modest than in the Nilsson case. On the other hand, the HF basis pushes the dipole peaks at too high energy with respect to experiments. A similar result was found in higher RPA calculations [36,37].

The $E2$ peaks fall at too high energy with respect to experiments whether a Nilsson or a HF basis is adopted. In fact, the lowest 2^+ states, having a multiphonon nature, can be pushed down in energy only by coupling the two-phonon components to the four-phonon subspace. Enlarging the space so as to include states with a number $n > 3$ of phonons is too time consuming unless we perform some drastic space truncation.

We have already cut the three-phonon states above some given energy. Apparently, the cut came out to be too severe, at least in the Nilsson basis. In fact, the three-phonon states taken into account were not sufficient to induce on the 1^- states a downward shift comparable to the one induced by the full two-phonon subspace on the ground state. Thus, the $E1$ peaks could not be brought back to the position obtained in TDA as required by the experiments. Increasing the number of three-phonon states becomes too time consuming for the configuration space we used and is prohibitive if such a space is enlarged.

We have therefore to try another route. We may select a restricted set of TDA phonons according to their energy and collectivity and use only them to construct a multiphonon basis. This option should allow us to incorporate an arbitrarily large number of ph states in the TDA phonons while including the multiphonon states of lowest energy and of collective character. The cut in the number of TDA phonons is also necessary in order to extend the multiphonon approach to heavy nuclei.

The present scheme is only suited to doubly magic nuclei. We have now formulated the method in terms of the Bogoliubov quasiparticle states so as to face the study of open shell nuclei. Its numerical implementation is completed and the results will be presented in a separate paper.

ACKNOWLEDGMENTS

We thank M. Hjorth-Jensen for useful information and stimulating discussions. The calculations were partly done at the MetaCentrum under the program "Projects of Large Infrastructure for Research, Development, and Innovations" LM2010005 funded by the Ministry of Education, Youth, and Sports of Czech Republic.

[1] P. F. Bortignon, A. Bracco, and R. A. Broglia, *Giant Resonances* (Harwood Academic Publishers, Amsterdam, 1998).
[2] M. Kneissl, N. Pietralla, and A. Zilges, J. Phys. G: Nucl. Part. Phys. **32**, R217 (2006).
[3] N. Pietralla, P. von Brentano, and A. F. Lisetskiy, Prog. Part. Nucl. Phys. **60**, 225 (2008).
[4] T. Auman, P. F. Bortignon, and H. Hemling, Annu. Rev. Nucl. Part. Sci. **48**, 351 (1998).
[5] J. Sawicki, Phys. Rev. **126**, 2231 (1962).
[6] C. Yannouleas, M. Dworzecka, and J. J. Griffin, Nucl. Phys. A **397**, 239 (1983).
[7] B. Schwesinger and J. Wambach, Phys. Lett. B **134**, 29 (1984).
[8] P. Papakonstantinou and R. Roth, Phys. Lett. B **671**, 356 (2009).
[9] A. Bohr and B. R. Mottelson, *Nuclear Structure*, Vol. II (Benjamin, New York, 1975), and references therein.
[10] J. S. Dehesa, S. Krewald, J. Speth, and A. Faessler, Phys. Rev. C **15**, 1858 (1977).
[11] P. F. Bortignon and R. A. Broglia, Nucl. Phys. A **371**, 405 (1981).
[12] J. Wambach, V. K. Mishra, and L. Chu-Hsia, Nucl. Phys. A **380**, 285 (1981).
[13] D. Gambacurta, M. Grasso, and F. Catara, Phys. Rev. C **81**, 054312 (2010).
[14] D. Gambacurta, M. Grasso, and F. Catara, Phys. Rev. C **84**, 034301 (2011).
[15] E. Litvinova, P. Ring, and V. I. Tselyaev, Phys. Rev. C **75**, 064308 (2007).
[16] E. Litvinova, P. Ring, and D. Vretenar, Phys. Lett. B **647**, 111 (2007).
[17] S. Kamerdzhiev, J. Speth, and G. Tertychnya, Phys. Rep. **393**, 1 (2004).
[18] E. Litvinova, P. Ring, and V. Tselyaev, Phys. Rev. C **78**, 014312 (2008).
[19] E. Litvinova, P. Ring, and V. Tselyaev, Phys. Rev. Lett. **105**, 022502 (2010).
[20] V. I. Tselyaev, Yad. Fiz. **50**, 1252 (1989) [Sov. J. Nucl. Phys. **50**, 780 (1989)].
[21] V. I. Tselyaev, Phys. Rev. C **75**, 024306 (2007).
[22] V. G. Soloviev, *Theory of Atomic Nuclei: Quasiparticles and Phonons* (Institute of Physics, Bristol, 1992).
[23] A. Tamii *et al.*, Phys. Rev. Lett. **107**, 062502 (2011).
[24] F. Andreozzi, F. Knapp, N. Lo Iudice, A. Porrino, and J. Kvasil, Phys. Rev. C **75**, 044312 (2007).
[25] F. Andreozzi, F. Knapp, N. Lo Iudice, A. Porrino, and J. Kvasil, Phys. Rev. C **78**, 054308 (2008).
[26] J. B. French, in *Proceedings of the International School of Physics Enrico Fermi, Course XXXVI*, Varenna 1965, edited by C. Bloch (Academic Press, New York and London, 1966), p. 279.
[27] M. Hjorth-Jensen, T. T. Kuo, and E. Osnes, Phys. Rep. **261**, 125 (1995).
[28] T. Engeland, M. Hjorth-Jensen, and G. R. Jansen, Computational environment for nuclear structure (CENS), [http://folk.uio.no/mhjensen/cp/software.html].
[29] R. Machleidt, Phys. Rev. C **63**, 024001 (2001).

[30] S. V. Nilsson and I. Ragnarsson, *Shape and Shells in Nuclear Structure* (Cambridge University Press, Cambridge, 1995).
[31] F. Palumbo, Nucl. Phys. **99**, 100 (1967).
[32] D. H. Glockner and R. D. Lawson, Phys. Lett. B **53**, 313 (1974).
[33] JENDL Photonuclear Data File 2004 (JENDL/PD-2004), [http://wwwndc.jaea.go.jp/jendl/jendl.html].
[34] W. C. Haxton and C. J. Johnson, Phys. Rev. Lett. **65**, 1325 (1990).
[35] P. Navratil, J. P. Vary, and B. R. Barrett, Phys. Rev. Lett. **84**, 5728 (2000).
[36] N. Paar, P. Papakonstantinou, H. Hergert, and R. Roth, Phys. Rev. C **74**, 014318 (2006).
[37] P. Papakonstantinou, R. Roth, and N. Paar, Phys. Rev. C **75**, 014310 (2007).